第 49 卷 第 22 期/2022 年 11 月/中国激光 研究论文

中国激光

AZ31B 镁合金可调环形光斑光纤激光焊接试验研究

张明军，吴乐峰，毛聪，张健，王开明，胡永乐，李河清*

长沙理工大学汽车与机械工程学院机械装备高性能智能制造关键技术湖南省重点实验室，湖南 长沙 410114

摘要 针对镁合金激光焊接焊缝成形和接头性能差的问题，提出了可调环形光斑光纤激光焊接新工艺。对 5 mm 厚的 AZ31B 镁合金对接接头进行了焊接试验，研究了中心激光束和环形激光束功率组合对焊缝宏观成形、显微组织和力学性能的影响规律。结果表明，当中心激光束功率大于环形激光束功率时，施加环形激光束可以显著增大焊缝上部的熔宽；当中心激光束功率小于环形激光束功率时，焊缝上表面和下表面成形均不稳定。在中心激光束作用区域，焊缝熔合线附近未见明显的热影响区和柱状晶区，且等轴晶晶粒较细。在环形激光束作用区域，焊缝熔合线附近存在热影响区和柱状晶区，且等轴晶晶粒粗大。随着环形激光束功率的增大，焊缝中心区的硬度值减小。当中心激光束的功率为 2000 W、环形激光束的功率为 1000 W 时，接头抗拉强度和延伸率最高，接头断裂于焊缝熔合线附近，呈韧-脆混合断裂模式。

关键词 激光技术；激光焊接；可调环形光斑光纤激光；AZ31B 镁合金；焊缝成形；显微组织

中图分类号 TG 456.7 **文献标志码** A **DOI**：10.3788/CJL202249.2202002

1 引 言

交通工具、航空、航天和国防军事装备构件等对轻量化的需求愈加迫切[1]。镁合金具有比强度和比刚度高、阻尼减振、电磁屏蔽以及优异的切削加工性能和易回收利用等优点。随着镁合金新材料、新技术的不断研发与创新，其应用潜力不可估量[2]。

镁合金常见的焊接方法有电弧焊[3-4]、搅拌摩擦焊[5-8]、激光焊[9-11]和激光-电弧复合焊[12-13]。然而，电弧焊存在焊接速度慢、热输入大和残余应力大等突出问题；搅拌摩擦焊工艺过程复杂、接头处易产生各向异性；激光焊具有速度快、热影响区小、熔深大等优点，成为镁合金熔焊连接的研究焦点[14-15]。刘黎明等[16-17]研究发现，激光-TIG 复合热源焊接（TIG，钨极惰性气体）可增加焊缝深度，提高焊接稳定性，并可获得性能优良的焊缝接头。单际国等[18]研究发现，预热及添加对接夹层材料可以在一定程度上抑制镁合金焊接接头的气孔。Gao 等[19-20]针对 AZ31B 变形镁合金，采用光纤激光-MIG 复合焊接（MIG，熔化极惰性气体）和 CO_2 脉冲激光-MIG 复合焊，获得了较好的焊接接头。Hao 等[11]采用光纤激光摆动焊焊接了 AZ31B 镁合金，结果表明，在摆动频率为 50 Hz 和摆动半径为 0.5 mm 时，焊缝成形最好。Lei 等[21]利用超声辅助激光焊接 AZ31B 镁合金，发现在超声波作用下，熔融区元素分布更均匀、晶粒尺寸明显变细，获得了强度较高的焊接接头。

最近，Duocastella 等[22]提出了一种将可调环形光斑应用于激光加工中的方法，引起了广泛关注。可调环形光斑由中心激光光斑和环形激光光斑组成，可以改善焊接质量[23-25]。Kang 等[23]采用可调环形光斑激光焊接铝合金，获得了焊接裂纹少且接头组织良好的焊接接头。Rinne 等[24]对钢-铜异种金属进行了可调环形光斑激光搭接焊，发现适当增大环形光斑激光功率可以改善焊缝成形和提高接头性能。Mohammadpour 等[25]指出可调环形光斑激光焊接可以提升低碳钢的焊接质量，中心激光和环形激光的功率匹配程度对焊缝成形和接头性能有较大影响。

综上所述，国内外学者对镁合金激光焊接开展了诸多研究工作，取得了较好的效果。然而，现有研究工作与实际工程应用还存在较大差距，新型激光焊接工艺技术亟待开发。本文采用可调环形光斑光纤激光焊接了 AZ31B 镁合金对接接头，对接头的表面成形、显微组织和力学性能进行了深入分析。

2 试验条件

图 1 为可调环形光斑光纤激光焊接试验装置图。试验采用的光纤激光器的中心激光功率最大为

收稿日期：2021-12-22；**修回日期**：2022-01-23；**录用日期**：2022-03-01

基金项目：湖南省教育厅科学研究项目（20B008）、长沙市自然科学基金（kq2014101）

通信作者：*liheqing2003@163.com

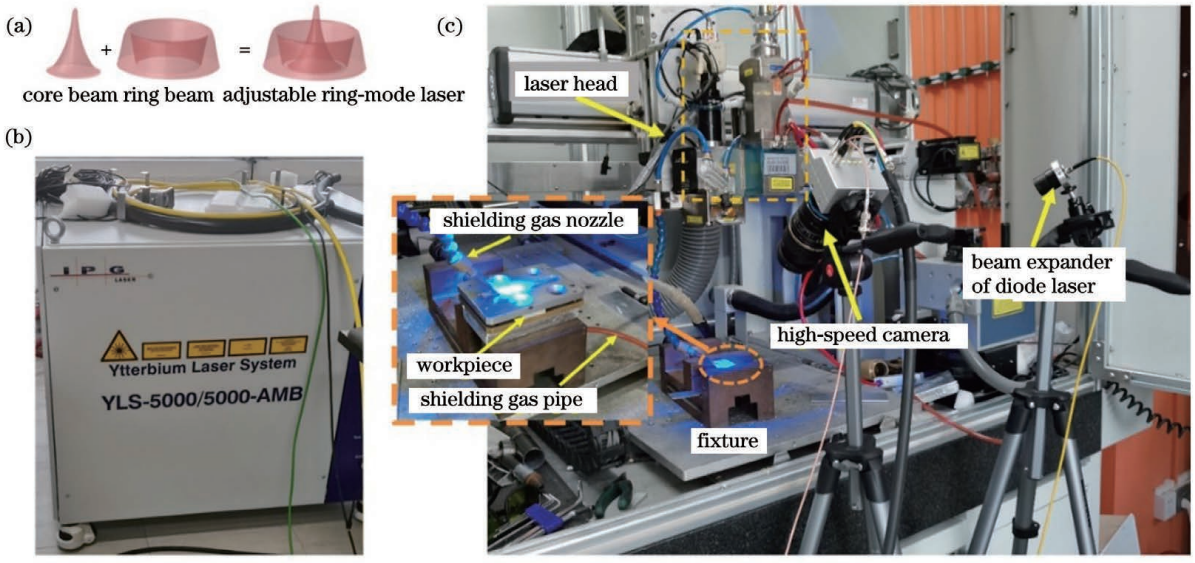

图 1 试验装置图。(a)可调环形光斑激光光束示意图;(b)光纤激光器;(c)现场布局图

Fig. 1 Experimental setup. (a) Schematic of laser beam with adjustable ring spot; (b) fiber laser; (c) in-site layout

5000 W,操作光纤芯径为 50 μm,环形激光功率最大为 5000 W,操作光纤芯径为 150 μm。两束激光通过焦距为 100 mm 的准直镜、焦距为 300 mm 的聚焦镜后,得到可调环形光斑,中心激光束和环形激光束的焦斑直径分别为 0.15 mm 和 0.45 mm。

试验用材料为轧制状态的5 mm厚AZ31B镁合金板材,尺寸为 50 mm×40 mm×5 mm,接头形式为对接,材料的化学成分如表 1 所示。焊前在试件表面上用钢刷和砂纸去除氧化皮并进行抛光,再用乙醇和丙酮擦拭干净。采用氩气作为上表面侧吹和背部保护气,侧吹气体和背部保护气体的流量均为 25 L/min。激光焊接工艺参数如表 2 所示。

表 1 AZ31B 镁合金的化学成分

Table 1 Chemical compositions of AZ31B magnesium alloy

Element	Al	Zn	Mn	Si	Fe	Cu	Ni	Mg
Mass fraction /%	2.960	0.520	0.310	0.160	0.003	0.006	0.001	Bal.

表 2 激光焊接工艺参数

Table 2 Laser welding process parameters

Specimen No.	Central laser power /W	Ring laser power /W	Welding speed /(mm/s)	Defocusing amount /mm
1#	3000	0	60	+2
2#	2000	1000		
3#	1500	1500		
4#	1000	2000		
5#	0	3000		

焊后采用体视镜对焊缝表面成形进行观察。然后采用电火花线切割方法截取拉伸和金相试样。采用 1 g 草酸、1 mL 乙酸、1 mL 硝酸加 150 mL 蒸馏水的配比配制腐蚀液,对经打磨抛光后的金相试样进行腐蚀,腐蚀时间为 15 s,干燥后在金相显微镜下观察焊缝微观组织。对焊缝中部位置(距焊缝上表面 2.5 mm)采用半自动维氏硬度计进行硬度测试,载荷为 100 g,保压时间为 10 s。拉伸试样的尺寸如图 2 所示,利用电子万能试验机进行焊接接头室温拉伸性能测试,加载速率为 0.5 mm/s,并采用电子扫描显微镜对拉伸断口进行观察。

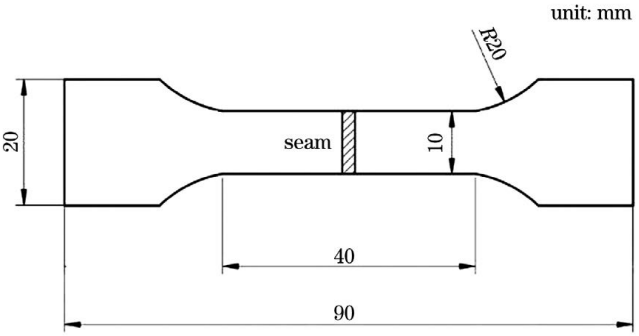

图 2 拉伸试样示意图

Fig. 2 Schematic of tensile specimen

3 试验结果与分析

3.1 可调环形光斑光纤激光对镁合金焊缝成形的影响

图 3 为不同激光功率组合下可调环形光斑激光焊缝宏观形貌图。利用 Image-pro 软件对焊缝上下表面熔宽、上表面塌陷量和下表面下掉量进行了测量。当仅有中心激光束且功率为 3000 W 时(1 # 试样),焊缝上表面和下表面分别出现连续塌陷和凹陷;上表面和下表面的熔宽窄且一致性好,呈 I 型焊缝,如图 3(a1)~(a3)和图 4 所示。此外,从焊缝成形特征可以看出,焊接模式为典型的小孔连续穿透模式[26]。当中心激光功率为 2000 W,环形激光功率为 1000 W 时(2 # 试样),焊缝上表面存在连续塌陷,但塌陷程度较 1 # 试样的小,下表面连续下掉,但下掉量较小;焊缝上表面熔宽较 1 # 试样的宽,下表面熔宽与 1 # 试样相当,呈 Y 型焊缝,如图 3(b1)~(b3)和图 4 所示。从焊缝成形特征可以看出,焊接模式为小孔连续穿透模式[26]。随着中心激光功率的下降,当环形激光的功率增加为 1500 W 或 2000 W 时,焊缝上表面出现周期性的塌陷,下表面连续下掉,但下掉量随环形激光功率的增大而增大;焊缝上表面和下表面的熔宽均随环形激光功率的增大而增大,呈鼓形焊缝,如图 3(c1)~(d3)和图 4 所示。从焊缝成形特征可以看出,焊接模式为小孔间断穿透模式[27]。当仅有环形激光束且功率为 3000 W 时(5 # 试样),焊缝上表面塌陷,下表面连续下掉且下掉量较大,同时存在底部驼峰;焊缝上表面和下表面熔宽相当,下表面熔宽在所有焊缝中是最宽的,如图 3(e1)~(e3)与图 4 所示。从焊缝成形特征可以看出,焊接模式为熔池熔透模式[27]。综上所述,环形激光对焊缝成形有显著影响。一方面,当中心激光功率大于环形激光功率时,施加环形激光可以显著增大焊缝上部的熔宽;中心和环形激光组合对焊缝横截面形貌的影响较大,当中心激光和环形激光功率分别为 2000 W 和 1000 W 时(2 # 试样),焊缝成形最佳。另一方面,当中心激光功率小于环形激光功率时,焊缝上表面和下表面成形均不稳定。

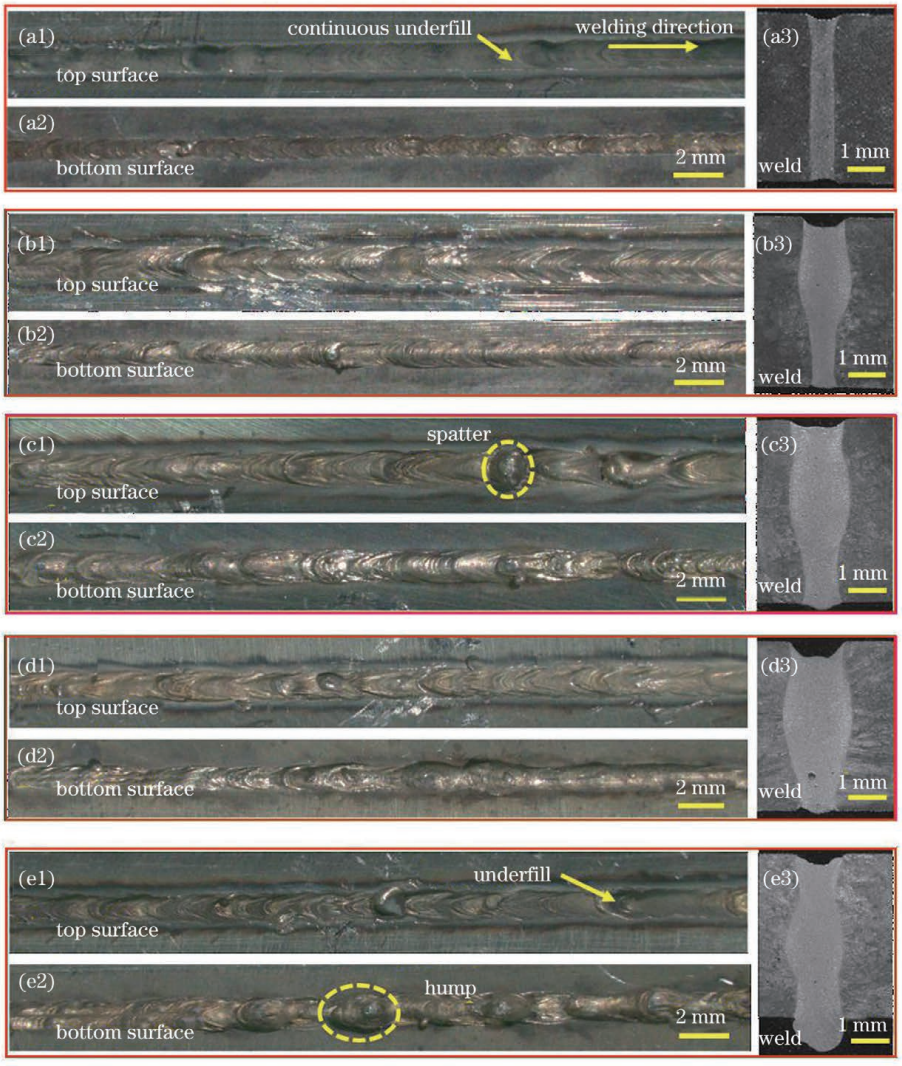

图 3 焊缝宏观形貌。(a1)~(a3)1 #;(b1)~(b3)2 #;(c1)~(c3)3 #;(d1)~(d3)4 #;(e1)~(e3)5 #

Fig. 3 Macro-morphologies of welds. (a1)-(a3) 1 #; (b1)-(b3) 2 #; (c1)-(c3) 3 #; (d1)-(d3) 4 #; (e1)-(e3) 5 #

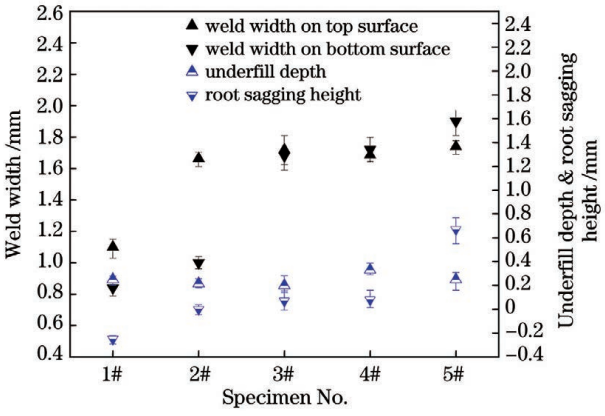

图 4　激光功率组合对焊缝熔宽和塌陷深度的影响

Fig. 4　Effects of laser power combination on weld width and underfill depth

3.2　可调环形光斑光纤激光对镁合金接头显微组织的影响

图 5 为焊缝显微组织形貌图。可以看出，母材的组织由 α-Mg、Mg-Al 化合物颗粒相组成。α-Mg 为等轴晶，大小不均匀，呈典型的挤压组织特征。从图 5(a1)～(a4)可以看出，当仅有中心激光束且功率为 3000 W 时(1＃试样)，焊缝熔合线附近的柱状晶区域很窄[图5(a2)]，等轴晶晶粒尺寸较小[图5(a3)]。这是由于小孔穿透型激光焊接过程中熔池小，熔融金属冷却速度快。此外，可以看到焊缝中存在小气孔且其周围出现裂纹[图 5(a4)]。当中心激光功率为 2000 W 和环形激光功率为 1000 W 时(2＃试样)，焊缝上部熔合线附近出现较宽的柱状晶区域[图 5(b2)]，焊缝中心等轴晶的尺寸也较小[图 5(b3)]，而焊缝底部熔合线附近的柱状晶区域很窄[图 5(b4)]，与 1＃试样类似。由此可知，此时环形激光束的作用区域主要集中在焊接熔池的上部，增大了熔池上部的熔化面积，从而延长了熔池上部的对流换热时间，进而在焊缝熔合线附近形成了较宽的柱状晶区[28]。同样地，焊缝中心上部区域的等轴晶由于受到更大热输入的影响，晶粒尺寸大于焊缝下部，如图 5(b5)所示。值得一提的是，上述焊缝熔合区边界处的热影响区不明显且没有热区组织粗大现象[14]。当仅有环形激光束且功率为 3000 W 时(5＃试样)，焊缝熔合线附近出现热影响区[图 5(c2)]，宽度约为 30 μm。焊缝中心分布大量的等轴晶，且晶粒尺寸较大，如图 5(c3)所示。这是由于熔池熔透模式下的焊接熔池体积较大，熔融金属的冷却凝固速率比小孔穿透型焊接模式小，因此焊缝区的晶粒粗大[29]。

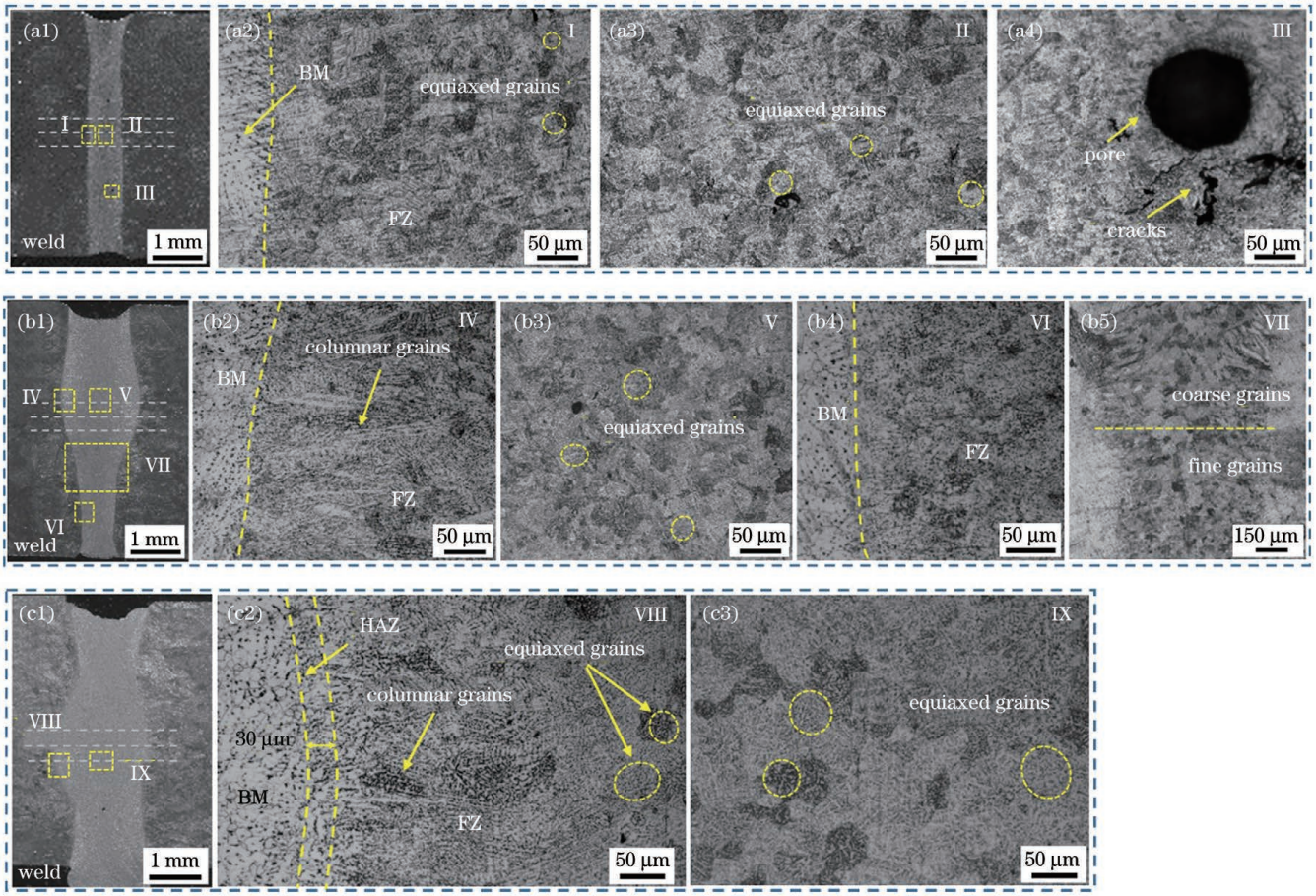

图 5　焊缝显微组织。(a1)～(a4)1＃；(b1)～(b5)2＃；(c1)～(c3)5＃

Fig. 5　Microstructures of welds. (a1)-(a4) 1＃; (b1)-(b5) 2＃; (c1)-(c3) 5＃

3.3 可调环形光斑光纤激光对镁合金接头力学性能的影响

图 6 为焊缝显微硬度分布图，其中 FZ 表示焊缝熔合区。沿焊缝横截面熔深中间位置的水平线测量显微硬度值，测量点的间距为 0.3 mm，在竖直方向上测量三处，取其平均值，如图 5(a1)、(b1)、(c1)水平虚线所示。可以看出，焊缝区的硬度值比母材区(64.9 HV)高，这是由于焊缝区的等轴晶晶粒较母材区细小。当仅有中心激光束且功率为 3000 W 时(1＃试样)，焊缝区的硬度值较大，平均值为 73.7 HV。当中心激光功率为 2000 W 和环形激光功率为 1000 W 时(2＃试样)，焊缝中心的硬度值大于 1＃试样。随着环形激光功率的增大，焊缝中心区的硬度值下降，仅环形激光焊接时(5＃试样)焊缝中心区的硬度值最小。这是由于环形激光功率越大，焊缝中心的等轴晶组织越粗大，从而焊缝中心的硬度值越小。

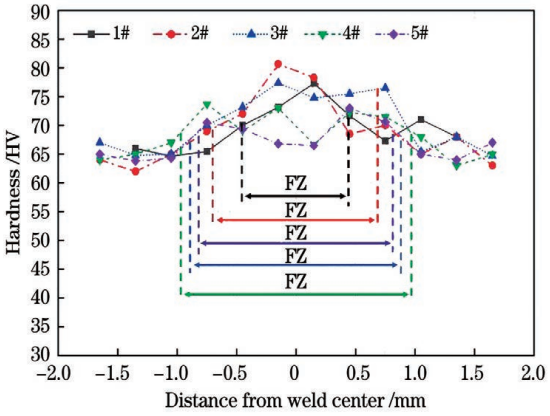

图 6 焊缝的显微硬度分布

Fig. 6 Microhardness distribution of weld

图 7 为焊缝接头的拉伸试验结果图，其中 BM 表示母材。从图 7(a)可以看出，AZ31B 镁合金母材的抗拉强度为 270 MPa，延伸率为 14.5%。当仅有中心激光束且功率为 3000 W 时(1＃试样)，焊接接头的抗拉强度和延伸率分别为 191 MPa 和 9.8%，为母材的 70.7%和 67.6%。当中心激光功率为 2000 W 和环形激光功率为 1000 W 时(2＃试样)，焊接接头的抗拉强度和延伸率最大，分别达到 215 MPa 和 14.0%，为母材的79.6%和96.6%。当仅有环形激光束且功率为 3000 W 时(5＃试样)，焊接接头的抗拉强度最低，为 176 MPa，是母材的 65.1%；但延伸率仅次于 2＃试样，达到 13.0%，为母材的 89.7%。由此可知，环形激光束的加入可以改善镁合金激光焊接头的延伸率，且在优化工艺参数下可以得到抗拉强度和延伸率最佳的焊缝接头。此外，拉伸性能最佳的 2＃试样是从焊缝熔合线附近开始断裂的，然后向母材扩展，最后在焊缝中心完全断裂。其余试件都是从焊缝中心开始断裂的，断口大部分位于焊缝区域之内，如图 7(b)所示。

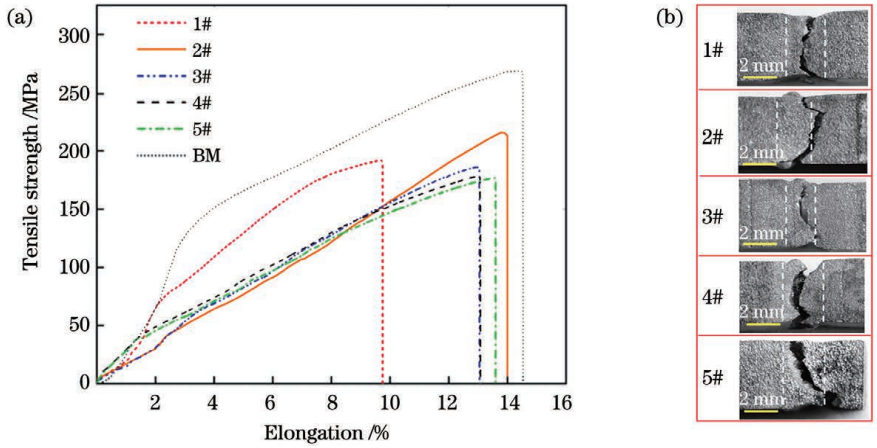

图 7 试件的拉伸试验结果。(a)拉伸曲线；(b)断口形貌

Fig. 7 Tensile test results of specimens. (a) Tensile curves; (b) fracture morphologies

图 8 为典型焊接接头的拉伸断口形貌。图 8(a1)、(a2)为母材断口形貌，有许多解理和准解理特征，也存在一些韧窝。在 1＃、2＃和 5＃断口处均观察到了若干解理面、准解理面特征和韧窝。此外，在 2＃断口处观察到的韧窝数量较 5＃多且尺寸更大，这说明 2＃断口的韧性比 5＃好，如图 8(c1)～(d2)所示。由此可知，可调环形光斑光纤激光焊接接头的拉伸断口韧性适中，接头呈脆性-韧性混合断裂[30]。

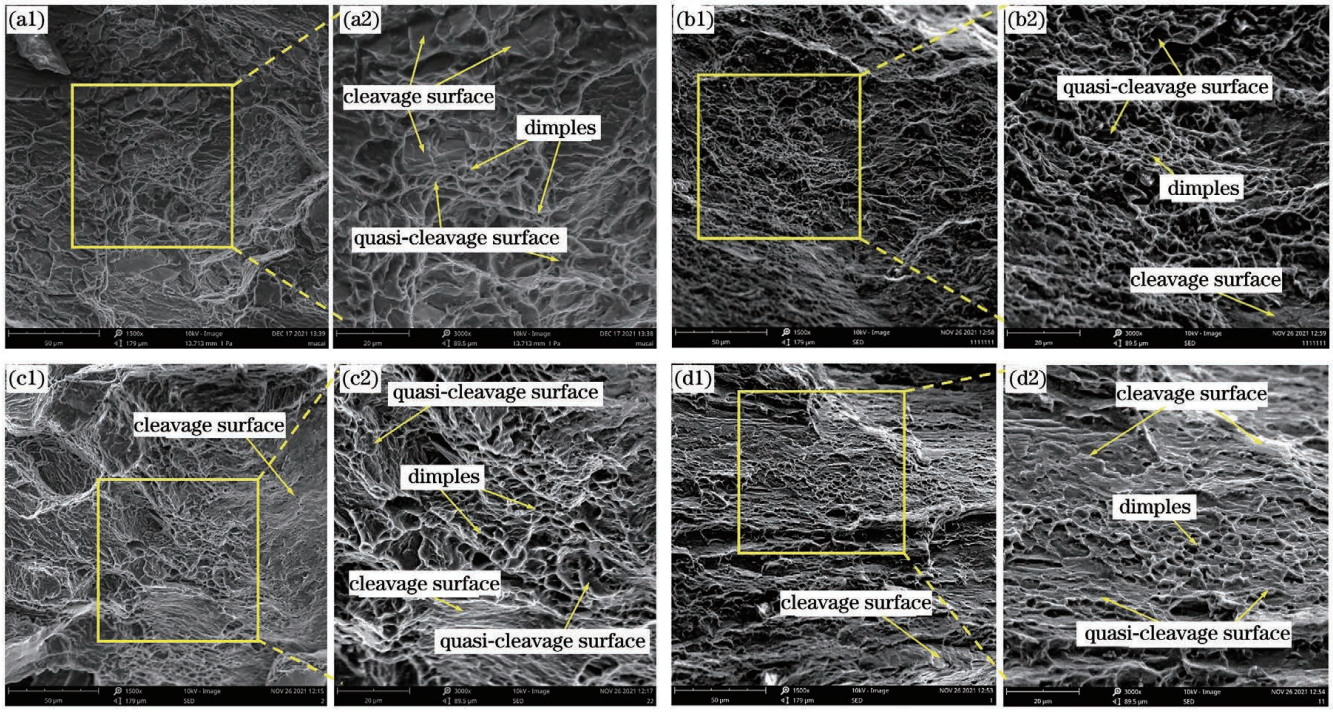

图 8 典型拉伸断口形貌。(a1)(a2)母材;(b1)(b2)1#;(c1)(c2)2#;(d1)(d2)5#

Fig. 8 Typical tensile fracture morphologies. (a1)(a2) Base metal; (b1)(b2) 1#; (c1)(c2) 2#; (d1)(d2) 5#

4 结 论

采用可调环形光斑光纤激光焊接 AZ31B 镁合金对接接头,研究了中心激光束和环形激光束功率组合对焊缝宏观成形、显微组织和力学性能的影响。主要结论如下:

1) 环形激光的存在对焊缝成形具有显著影响。当中心激光功率大于环形激光功率时,施加环形激光可以显著增大焊缝上部的熔宽。中心和环形激光组合对焊缝横截面形貌的影响较大,当中心激光和环形激光功率分别为 2000 W 和 1000 W 时,焊缝成形最佳。当中心激光功率小于环形激光功率时,焊缝上表面和下表面成形均不稳定。

2) 环形激光的存在对焊缝显微组织有一定的影响。在仅中心激光作用的区域,焊缝熔合线附近未见明显的热影响区和柱状晶区,且等轴晶晶粒较细。在环形激光作用的区域,焊缝熔合线附近存在热影响区和柱状晶区,且等轴晶晶粒粗大。随着环形激光功率的增大,焊缝中心区的硬度值下降。

3) 当中心激光功率为 2000 W 和环形激光功率为 1000 W 时,接头抗拉强度和延伸率最高,接头从焊缝熔合线附近开始断裂,呈韧-脆混合断裂模式。环形激光束的加入可以改善镁合金激光焊接头的延伸率,且在优化工艺参数下可以得到抗拉强度较好的焊缝接头。

参 考 文 献

[1] 刘金钊, 颜廷艳, 康绪枫, 等. 激光功率对双激光束双侧同步焊接 TC4 钛合金 T 型接头断裂性能的影响机理[J]. 中国激光, 2021, 48(18): 1802007.
Liu J Z, Yan T Y, Kang X F, et al. Influence of laser power on fracture properties of TC4 titanium alloy T-joint manufactured using dual-laser-beam bilateral synchronous welding[J]. Chinese Journal of Lasers, 2021, 48(18): 1802007.

[2] 张书迈, 张福全, 周惦武, 等. Ni 夹层对镁合金/铝合金激光熔焊接头组织和性能的影响[J]. 中国激光, 2020, 47(7): 0702001.
Zhang S M, Zhang F Q, Zhou D W, et al. Effects of Ni interlayer on microstructure and properties of fusion welded joints of magnesium/aluminum alloys[J]. Chinese Journal of Lasers, 2020, 47(7): 0702001.

[3] Guo Y Y, Quan G F, Jiang Y L, et al. Formability, microstructure evolution and mechanical properties of wire arc additively manufactured AZ80M magnesium alloy using gas tungsten arc welding[J]. Journal of Magnesium and Alloys, 2021, 9(1): 192-201.

[4] Xu N, Shen J, Xie W D, et al. Abnormal distribution of microhardness in tungsten inert gas arc butt-welded AZ61 magnesium alloy plates[J]. Materials Characterization, 2010, 61(7): 713-719.

[5] Wang X P, Morisada Y, Fujii H. Interface development and microstructure evolution during double-sided friction stir spot welding of magnesium alloy by adjustable probes and their effects on mechanical properties of the joint[J]. Journal of Materials Processing Technology, 2021, 294: 117104.

[6] Zhang H F, Zhou L, Li W L, et al. Effect of tool plunge depth on the microstructure and fracture behavior of refill friction stir spot welded AZ91 magnesium alloy joints[J]. International Journal of Minerals, Metallurgy and Materials, 2021, 28(4): 699-709.

[7] 袁胜男, 王快社, 乔柯, 等. 搅拌摩擦加工制备 AZ31/ZrO_2 复合材料的组织性能研究[J]. 塑性工程学报, 2021, 28(3): 190-197.
Yuan S N, Wang K S, Qiao K, et al. Microstructure and properties of AZ31/ZrO_2 composites prepared by friction stir processing[J]. Journal of Plasticity Engineering, 2021, 28(3): 190-197.

[8] 侯晶, 秦鼎强, 毛悦, 等. 镁合金高转速搅拌摩擦焊工艺研究

[J]. 精密成形工程, 2019, 11(6): 127-134.
Hou J, Qin D Q, Mao Y, et al. High speed friction stir welding process of magnesium alloy[J]. Journal of Netshape Forming Engineering, 2019, 11(6): 127-134.
[9] 戎易, 程东海, 熊震宇, 等. 交变磁场辅助添加镍中间层镁/钢激光熔钎焊接头的组织性能研究[J]. 中国激光, 2021, 48(22): 2202005.
Rong Y, Cheng D H, Xiong Z Y, et al. Microstructure and properties of laser welding-brazing welded joint of Mg/steel with Ni interlayer assisted by alternating magnetic field[J]. Chinese Journal of Lasers, 2021, 48(22): 2202005.
[10] Lei Z L, Bi J, Li P, et al. Analysis on welding characteristics of ultrasonic assisted laser welding of AZ31B magnesium alloy[J]. Optics & Laser Technology, 2018, 105: 15-22.
[11] Hao K D, Wang H K, Gao M, et al. Laser welding of AZ31B magnesium alloy with beam oscillation[J]. Journal of Materials Research and Technology, 2019, 8(3): 3044-3053.
[12] 宋刚, 于培妮, 李涛涛, 等. 镁合金/钢激光诱导电弧复合焊接模拟及分析[J]. 中国激光, 2020, 47(6): 0602001.
Song G, Yu P N, Li T T, et al. Simulation and analysis of magnesium alloy/steel by laser-induced arc hybrid welding[J]. Chinese Journal of Lasers, 2020, 47(6): 0602001.
[13] 辛立军, 林三宝, 刘旭平等. 激光-电弧复合焊接镁合金过程中匙孔行为与气孔形成的关系[J]. 稀有金属材料与工程, 2020, 49(6): 1894-1900.
Xin L J, Lin S B, Liu X P, et al. Relationship between molten pool behavior and keyhole-induced porosity in pulsed laser-arc hybrid welding of magnesium alloy[J]. Rare Metal Materials and Engineering, 2020, 49(6): 1894-1900.
[14] 檀财旺, 李俐群, 陈彦宾, 等. AZ31B 镁合金的光纤激光与 CO_2 激光焊接特性[J]. 中国激光, 2011, 38(6): 0603015.
Tan C W, Li L Q, Chen Y B, et al. Characteristics of fiber laser and CO_2 laser welding of AZ31B magnesium alloys[J]. Chinese Journal of Lasers, 2011, 38(6): 0603015.
[15] 张高磊, 孔华, 邹江林, 等. 高功率光纤激光深熔焊接飞溅特性以及离焦量对飞溅的影响[J]. 中国激光, 2021, 48(22): 2202008.
Zhang G L, Kong H, Zou J L, et al. Spatter characteristics of high-power fibre laser deep penetration welding and effect of defocus on spatter[J]. Chinese Journal of Lasers, 2021, 48(22): 2202008.
[16] 刘黎明, 王继锋, 宋刚. 激光电弧复合焊接 AZ31B 镁合金[J]. 中国激光, 2004, 31(12): 1523-1526.
Liu L M, Wang J F, Song G. Hybrid laser-arc welding of AZ31B Mg alloy[J]. Chinese Journal of Lasers, 2004, 31(12): 1523-1526.
[17] 宋刚, 刘黎明, 王继锋, 等. 激光-TIG 复合焊接镁合金 AZ31B 焊接工艺[J]. 焊接学报, 2004, 25(3): 31-34, 130.
Song G, Liu L M, Wang J F, et al. Laser tungsten inert-gas arc hybrid welding process on wrought magnesium ahoy AZ31B[J]. Transactions of the China Welding Institution, 2004, 25(3): 31-34, 130.
[18] 单际国, 张婧, 郑世卿, 等. 镁合金激光焊接气孔问题的实验研究[J]. 稀有金属材料与工程, 2009, 38(S3): 234-239.
Shan J G, Zhang J, Zheng S Q, et al. Experimental study on pores in laser welding of magnesium alloys[J]. Rare Metal Materials and Engineering, 2009, 38(S3): 234-239.
[19] Gao M, Tang H G, Chen X F, et al. High power fiber laser arc hybrid welding of AZ31B magnesium alloy[J]. Materials & Design, 2012, 42: 46-54.
[20] Gao M, Mei S W, Wang Z M, et al. Process and joint characterizations of laser-MIG hybrid welding of AZ31 magnesium alloy[J]. Journal of Materials Processing Technology, 2012, 212(6): 1338-1346.
[21] Lei Z L, Bi J, Li P, et al. Melt flow and grain refining in ultrasonic vibration assisted laser welding process of AZ31B magnesium alloy[J]. Optics & Laser Technology, 2018, 108: 409-417.
[22] Duocastella M, Arnold C B. Bessel and annular beams for materials processing[J]. Laser & Photonics Reviews, 2012, 6(5): 607-621.
[23] Kang M, Kim C. Evaluation of hot cracking susceptibility on laser welded aluminum alloy using coaxially arranged multiple-beam laser [J]. Journal of Laser Applications, 2020, 32(2): 022072.
[24] Rinne J S, Nothdurft S, Hermsdorf J, et al. Advantages of adjustable intensity profiles for laser beam welding of steel copper dissimilar joints[J]. Procedia CIRP, 2020, 94: 661-665.
[25] Mohammadpour M, Wang L, Kong F R, et al. Adjustable ring mode and single beam fiber lasers: a performance comparison [J]. Manufacturing Letters, 2020, 25: 50-55.
[26] Zhang M J, Tang K, Zhang J, et al. Effects of processing parameters on underfill defects in deep penetration laser welding of thick plates [J]. The International Journal of Advanced Manufacturing Technology, 2018, 96(1/2/3/4): 491-501.
[27] Zhang M J, Zhang Y Z, Mao C, et al. Experiments on formation mechanism of root humping in high-power laser autogenous welding of thick plates with stainless steels [J]. Optics & Laser Technology, 2019, 111: 11-19.
[28] Lin C M, Tsai H L, Lee C L, et al. Influence of CO_2 laser welding parameters on the microstructure, metallurgy, and mechanical properties of Mg-Al alloys[J]. International Journal of Minerals, Metallurgy, and Materials, 2012, 19(12): 1114-1120.
[29] Quan Y J, Chen Z H, Gong X S, et al. Effects of heat input on microstructure and tensile properties of laser welded magnesium alloy AZ31 [J]. Materials Characterization, 2008, 59(10): 1491-1497.
[30] Wang L Z, Shen J, Xu N. Effects of TiO_2 coating on the microstructures and mechanical properties of tungsten inert gas welded AZ31 magnesium alloy joints[J]. Materials Science and Engineering: A, 2011, 528(24): 7276-7284.

Experimental Research on AZ31B Magnesium Alloy Welded Using Fiber Laser with Adjustable Ring Spot

Zhang Mingjun, Wu Lefeng, Mao Cong, Zhang Jian, Wang Kaiming, Hu Yongle, Li Heqing*

Hunan Provincial Key Laboratory of Key Technologies for High-Performance Intelligent Manufacturing of Mechanical Equipment, College of Automotive and Mechanical Engineering, Changsha University of Science and Technology, Changsha 410114, Hunan, China

Abstract

Objective For transportation, aviation, aerospace, and defense military equipment components, the need for

lightweighting is particularly urgent. Magnesium alloys have the benefits of high specific strength and stiffness, damping and vibration reduction, electromagnetic shielding, remarkable machining performance, and easy recycling. With the continuous research and innovation of new materials and technologies of magnesium alloys, their application potential will be infinite. Researchers suggested an approach of applying a tunable ring spot in laser processing that has attracted a lot of attention in the field of laser processing. Although domestic and foreign scholars have performed a lot of research investigations on magnesium alloy laser welding and have attained good findings. There is still a big gap between the existing research investigations and practical engineering applications, and it is crucial to develop novel laser welding technology.

Methods In this study, AZ31B magnesium alloy butt joints with a thickness of 5 mm are welded by fiber laser with an adjustable ring spot. Based on ensuring the total power of 3 kW, pure center laser, center laser/ring laser, and pure ring laser are employed to weld magnesium alloy joints. The surface shapes, microstructures, and mechanical properties of the joints are discovered and examined.

Results and Discussions In terms of weld formation, first, compared with that when using pure center laser welding, the melting width in the upper part of the weld is considerably increased when using ring laser welding, and the combination of center laser and ring laser has a greater impact on the weld cross-sectional shape. Second, when the ring laser power is greater than the center laser power, the formations of the upper and lower surfaces of the welds become unstable (Figs. 3 and 4). In terms of metallographic structure, during pure center laser welding, the columnar crystal region near the fusion line of the weld is very narrow, and the grains in the center of the weld are finer, but due to the fast cooling rate, there are small pores and cracks around the weld [Figs. 5(a1)–(a4)]. When the center is welded with a ring laser, the convection heat transfer time is extended in the molten pool's upper part, increasing the grain size in the center of the weld. Even in pure annular laser welding, a wide columnar grain region is formed near the weld fusion line [Figs. 5(c1)–(c3)]. The weld zone hardness is higher than that of the base metal, and as the ring laser power increases, the weld center hardness decreases. When the central laser power is 2000 W and the ring laser power is 1000 W (sample 2#), the tensile strength and elongation of the welded joint are the largest, reaching 215 MPa and 14.0%, respectively, which are 79.6% and 96.6% of those of the base metal [Fig. 7(a)]. The joint fracture is a brittle-ductile mixed fracture.

Conclusions The existence of a ring laser has a considerable influence on the weld formation. Based on the center laser, the ring laser application can substantially increase the fusion width in the upper part of the weld. The combination of center laser and ring laser has a great influence on the cross-sectional shape of the weld, the best weld formation is generated when the center laser power is 2000 W and the ring laser power is 1000 W. The existence of ring laser has a certain effect on the microstructure of the weld. Only in the central laser action area, there is no clear heat-affected zone or columnar grain zone near the weld fusion line, and the equiaxed grains are relatively fine. In the ring laser action area, there are heat-affected and columnar crystal zones near the weld fusion line, and the equiaxed crystal grains are coarse. Further, with the ring laser power increasing, the hardness value of the central area of the weld decreases. The ring laser beam can enhance the elongation of laser welded joints of the magnesium alloys, and the welded joints have better tensile strength produced under the optimized process parameters.

Key words laser technique; laser welding; fiber laser with adjustable ring spot; AZ31B magnesium alloy; weld appearance; microstructure